Developmental Cell
Article

# Apical Secretion in Epithelial Tubes of the *Drosophila* Embryo Is Directed by the Formin-Family Protein Diaphanous

R'ada Massarwa,[1] Eyal D. Schejter,[1] and Ben-Zion Shilo[1,*]
[1]Department of Molecular Genetics, Weizmann Institute of Science, Rehovot 76100, Israel
*Correspondence: benny.shilo@weizmann.ac.il
DOI 10.1016/j.devcel.2009.04.010

## SUMMARY

**Apical localization of filamentous actin (F-actin) is a common feature of epithelial tubes in multicellular organisms. However, its origins and function are not known. We demonstrate that the Diaphanous (Dia)/Formin actin-nucleating factor is required for generation of apical F-actin in diverse types of epithelial tubes in the *Drosophila* embryo. Dia itself is apically localized both at the RNA and protein levels, and apical localization of its activators, including Rho1 and two guanine exchange factor proteins (RhoGEFs), contributes to its activity. In the absence of apical actin polymerization, apical-basal polarity and microtubule organization of tubular epithelial cells remain intact; however, secretion through the apical surface to the lumen of tubular organs is blocked. Apical secretion also requires the Myosin V (MyoV) motor, implying that secretory vesicles are targeted to the apical membrane by MyoV-based transport, along polarized actin filaments nucleated by Dia. This mechanism allows efficient utilization of the entire apical membrane for secretion.**

## INTRODUCTION

Tubular epithelial networks are an essential component of the body plan in all multicellular organisms. Branched tubular structures evolved to transfer solutes, hormones, nutrients, waste products, and air between tissues, thereby facilitating growth of the organism. Several features are common to all tubular structures, despite their distinct functions. The tube cells are highly polarized, such that the protein and lipid composition of the apical membrane facing the lumen is distinct from the basolateral domain that is attached to the extracellular matrix. The epithelial cells comprising the tube wall form junctions that are essential for maintaining tube integrity, and provide a seal preventing leakage of substances from the lumen to the basolateral surface, and vice versa (Bryant and Mostov, 2008; Hogan and Kolodziej, 2002; O'Brien et al., 2002).

Several mechanisms have been shown to generate polarity in epithelial tubes. In cases where the tubes are derived by invagination of polarized ectodermal cells (e.g., during formation of the *Drosophila* tracheal system or salivary glands, or the vertebrate lung), the original polarity is maintained during the formation and elaboration of the tube (Kerman et al., 2006; Lubarsky and Krasnow, 2003). Alternatively, cell clusters that are not yet polarized generate a lumen, as cells in the center of the cluster acquire apical-basal polarity (e.g., in the mammary gland and early pancreas bud) (Hogan and Kolodziej, 2002). Finally, polarized lumens may even be formed within a single cell. In the terminal cells of the *Drosophila* trachea, or in the excretory cell of *Caenorhabditis elegans*, coalescence and fusion of apical vesicles leads to the formation of a continuous, polarized, intracellular tube (Buechner et al., 1999; Ghabrial et al., 2003).

Generation and maintenance of the polarized tube structure, requires distinct trafficking mechanisms of secretory vesicles that will supply the different components to each membrane domain. Regulated apical secretion was shown to be responsible for stereotyped tube diameter expansion in the *Drosophila* trachea (Beitel and Krasnow, 2000; Hemphala et al., 2003) and salivary glands (Myat and Andrew, 2002). When the general secretory machinery was compromised by mutations in the COPII or COPI complexes, defects in luminal secretion of a variety of proteins were observed in the *Drosophila* tracheal system (Devine et al., 2005; Jayaram et al., 2008; Tsarouhas et al., 2007). Since many epithelial tubes are actively involved in secretion of substances to the lumen, efficient vectorial trafficking of secretory vesicles to the apical surface is essential, not only for generating and maintaining the tube, but also for carrying out the physiological function of the organ.

Tubular epithelial networks display considerable diversity in size and architecture, and secrete distinct components to the lumen. Yet the similarity in cellular epithelial organization raises the possibility that common mechanisms may be involved in apical secretion. One unifying feature that was identified is the concentration of filamentous actin (F-actin) at the apical surface of the cells comprising the tube. Such organization of actin was observed in cells forming the trachea of *Drosophila*, and in mammalian Madin-Darby canine kidney (MDCK) cells that are induced to form tubes in culture (O'Brien et al., 2002; Tsarouhas et al., 2007). This dense organization of actin is distinct from the actin that is typically associated with adherens junctions, as it is present under the entire apical surface. The nucleation machinery responsible for apical F-actin (commonly termed "the terminal web"), as well as its functional role, have not been well explored. It has been suggested that the terminal web contributes to the elastic properties of the cells lining the lumen. Dynamic alterations in the structure of the terminal web were observed upon stimulated secretion (e.g., in the lacrimal gland),

raising the possibility that it may either impede or facilitate regulated secretion to the lumen (Jerdeva et al., 2005; Wu et al., 2006).

In this work, we demonstrate that apical F-actin in epithelial tubes of the *Drosophila* embryo is generated by the Diaphanous (Dia)/Formin actin-nucleating factor. Formins constitute a diverse family of proteins found in all eukaryotes. They regulate nucleation of linear actin filaments, which give rise to protruding filipodia or intracellular actin filaments. Formins are involved in diverse cellular processes, including cytokinesis, cell migration utilizing filipodia, focal adhesions, polarized cell growth, stabilization of adherens junctions (Homem and Peifer, 2008), and microtubule stabilization (reviewed by Faix and Grosse [2006]). Dia-family formins are autoinhibited through intramolecular interactions. Upon binding to GTP-bound Rho GTPases, the Dia molecule assumes an open conformation and dimerizes. The Formin-homology domain 2 within the protein initiates actin filament assembly, and remains associated with the fast-growing barbed end, allowing rapid insertion of monomeric actin, while protecting the end from capping proteins (reviewed by Goode and Eck [2007]).

We show that the Dia-induced apical actin nucleation mechanism is common to several tubular structures, including the tracheal network, salivary glands, hindgut, and Malpighian tubules. In the absence of Dia, while the overall polarity of the cells and microtubule organization remains intact, apical F-actin is not formed. A complete block of secretion via the apical surface to the tube lumen is coupled to the loss of apical F-actin in all tubular organs examined, while proteins that are secreted to the lumen via septate junctions are not affected. Our data suggest that the apical restriction of Dia nucleating activity is a consequence of apical localization of the Dia-activating machinery, Rho1, and associated guanine exchange factors (GEFs), as well as of Dia itself. We further show that apical secretion requires the Myosin V (MyoV) motor protein, implying that secretory vesicles are targeted to the apical, lumen-facing membrane by MyoV-based transport along polarized actin filaments nucleated by Dia. This mechanism allows efficient utilization of the entire apical membrane for secretion, and appears to be general for distinct types of tubes, differing in their diameter, luminal composition, and physiological role.

## RESULTS

### Apical Filamentous Actin in Embryonic Tubular Networks Is Generated by Dia

We explored the distribution of F-actin in tubular structures of the *Drosophila* embryo using tissue-specific expression of the GFP-tagged F-actin binding domain of Moesin (Chihara et al., 2003), and observed a common apical localization. In the tracheal system, apical F-actin is first observed at stage 13 at the apical side of the cells forming the dorsal trunk. As the smaller tracheal tubes organize and form a lumen, F-actin appears (Figures 1A and 1C). F-actin was also detected apically in the hindgut, salivary glands, Malpighian tubules, and proventriculus (Figures 1B and 1D–1G).

To identify the molecular machinery responsible for formation of the apical layer of microfilaments in these tubular organs, we interfered with the function of several prominent F-actin nucleating systems. To study the requirement for Dia in this context, we examined both embryos homozygous for a strong loss-of-function allele of *dia* (where maternally provided *dia* transcripts allow the embryos to proceed normally through the first stages of embryogenesis, where Dia is required for other processes [Homem and Peifer, 2008]), as well as embryos in which *dia* RNAi constructs were expressed in tubular structures, using appropriate Gal4 drivers. Under both strategies, we observed loss of apical F-actin in the trachea, while residual F-actin in the adherens junctions was maintained (Figures 1H, 1J, 1M, and 1N). Maintenance of intact adherens junctions in the absence of Dia was also observed by the presence of Armadillo (Arm), and the electron-dense structures observed at the junctions in transmission electron microscopy (Figures 1I–1L). In contrast, inactivation of another actin-nucleation factor, the Arp2/3 complex, had no effect. Specifically, coexpression in the trachea of RNAi constructs for the *Sop2* and *Arp3* genes, encoding subunits of the Arp2/3 complex, did not alter the apical F-actin localization pattern (Figure 1O). When expressed in muscles, the same RNAi constructs phenocopied the Arp2/3 mutant phenotype (Massarwa et al., 2007), demonstrating their biological potency (Figures 1P–1Q). Similar results were obtained in the hindgut and salivary glands (see Figure S1 available online). These results demonstrate that Dia is essential for the formation of the apical F-actin web in the cells comprising the various tubes, and is likely to be the primary actin nucleator operating in this context.

To rule out the possibility that the absence of apical F-actin is a secondary consequence of disruptions to epithelial cell polarity, we monitored the localization pattern of different polarity markers in the *dia* mutant background. These markers included Crumbs (Crb), which localizes to the apical membrane, DE-Cadherin and Arm, which concentrate at adherens junctions, and Discs large (Dlg), which localizes to septate junctions (Figures 2A–2D). All markers exhibited normal localization in the tracheal tubes of *dia* mutant embryos (Figures 2E–2H), indicating that cell polarity is maintained. A similar conservation of cell polarity was observed in the hindgut and salivary glands of *dia*-mutant embryos (Figure S2).

Another hallmark of cell polarity, which impinges on targeted intracellular trafficking, is the organization of microtubules. The polarity of microtubules in *Drosophila* cells can be examined by Nod-lacZ, a microtubule minus-end-directed reporter (Clark et al., 1997). We find that Nod-lacZ is localized to the apical side of all embryonic epithelial tubes. Staining of microtubules by antibodies directed against β-tubulin demonstrates that Nod-lacZ is concentrated at the apical end of the domain harboring microtubules, indicating that microtubule polarization remained intact in the absence of Dia (Figures 2I and 2J; Figure S2). Taken together, these observations demonstrate that crucial aspects of epithelial cell polarity, including distinct membrane domains and microtubule organization, remain fully intact when Dia function is disrupted. The observed loss of apical F-actin in this background is thus likely to be a direct result of impaired Dia-nucleating activity.

### Dia mRNA and Protein Are Apically Localized

The apical concentration of F-actin generated by Dia prompted us to examine the basis for the apical focus of Dia activity. Dia displays a widespread and dynamic expression pattern during early and mid-stages of embryogenesis (data not shown).

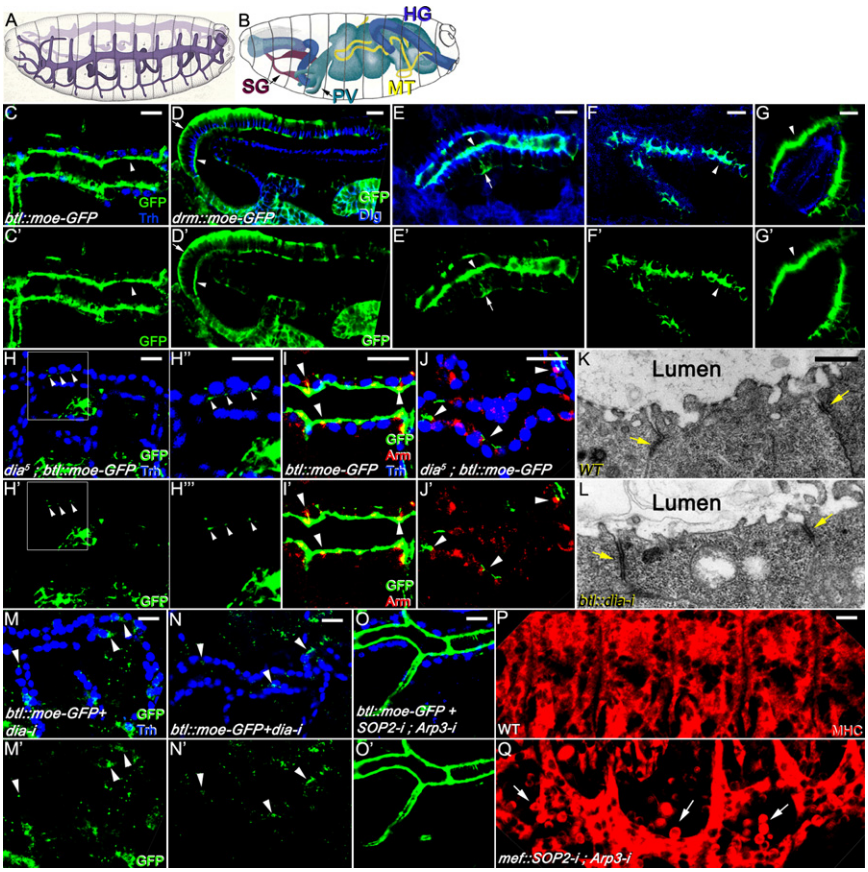


**Figure 1. Apical F-Actin in Tubular Epithelia Is Formed by Dia/Formin**

(A) Scheme of embryo at stage 14 showing the branched tracheal network comprised of polarized unicellular tubes that are interconnected.

(B) Scheme of a stage 16 embryo, showing the diverse tubular organs, including the hindgut (HG), salivary glands (SG), malpighian tubules (MT), and proventriculus (PV) (Hartenstein, 1993). In all subsequent panels, F-actin is marked by localization of Moe-GFP (green), which was expressed in the trachea by *btl-Gal4*, and in the hindgut, salivary glands, malpighian tubules, and proventriculus by *drm-Gal4*. In (C)–(G), arrowheads and arrows mark apical and basal surfaces, respectively.

(C) Dorsal trunk of trachea. Tracheal nuclei marked by Trachealess (Trh; blue).

(D) Hindgut: cell borders marked by Dlg (blue); F-actin shows both apical and basal concentrations.

(E) Salivary gland: Dlg, blue.

(F) Malpighian tubules: Dlg, blue.

(G) Proventriculus: Dlg, blue. This organ is comprised of two epithelial layers, where actin is observed on the apical side of the outer layer.

(H) In $dia^5$ zygotic mutant embryos, apical F-actin disappears, and is retained only in the adherens junctions (arrowheads).

(I and J) The position of Arm (red) in the adherens junctions in $dia^5$ mutants is comparable to wild-type, and colocalizes with the residual F-actin (arrowheads).

(K and L) Transmission electron microscopy analysis of a stage 15 embryo shows that, following expression of *dia* RNAi (VDRC20518) in the trachea, adherens junctions in the dorsal trunk are maintained, and are detected by electron-dense material (arrows). Scale bar, 0.5 μm.

(M and N) Loss of apical F-actin was also obtained following expression of RNAi for *dia* by *btl-Gal4* by using two nonoverlapping constructs (NIG1768R-1 or VDRC20518, respectively). Arrowheads show residual F-actin in adherens junctions. Scale bars, 10 μm.

(O) No alteration in apical F-actin in the trachea was observed following expression of RNAi constructs directed against the genes encoding Sop2 and Arp3 subunits of the Arp2/3 complex (VDRC42172, VDRC35260) by *btl-Gal4*. Scale bar, 10 μm.

(P and Q) Expression of the *Sop2* and *Arp3* RNAi constructs in muscles by *mef2-Gal4* mimicked the Arp2/3 muscle fusion phenotype (arrows), confirming their biological potency. (C′)–(J′) and (M′)–(O′) show only the F-actin (green) channel. Scale bar, 10 μm.

Scale bars, 10 μm (C–J).

However, from embryonic stage 14 and onward, *dia* mRNA is found predominantly within cells that form tubular structures, including the trachea, hindgut, salivary glands, Malpighian tubules, and the outer layer of the proventriculus (Figures 3A and 3B). Moreover, within each of these epithelial structures, the mRNA is tightly concentrated at the apical side (Figures 3C–3G). The apical localization of *dia* mRNA is mirrored at the protein level. Staining with anti-Dia antibodies shows that Dia protein persists in most tissues even during advanced stages of embryogenesis. At these stages, Dia protein exhibits a polarized apical localization specifically within the tubular structures, similar to *dia* mRNA, while a uniform distribution is observed in the other tissues (Figures 3H–3L). The activity of the *dia* RNAi construct could be demonstrated by disappearance of Dia protein in tissues where it was induced (Figure 3M).

To examine the mechanism for apical localization of *dia* mRNA and protein, we expressed a *dia-GFP* construct in which the 3′ untranslated region (UTR) was removed (Homem and Peifer, 2008). This mRNA, monitored in situ by a *GFP* probe, loses its apical localization (Figure 3N), demonstrating that the 3′UTR contains sequences required for apical targeting. However, the Dia-GFP protein remained apically localized, as determined by the GFP label (Figures 3O and 3P). Thus, a distinct apical targeting mechanism for the Dia protein, operating only within tubular epithelial cells, is sufficient for localization, even when the mRNA is uniformly distributed within these cells.

## Dia Is Required for Secretion to the Lumen of Tubular Organs

A central feature of tubular epithelial cells is their ability to secrete proteins to the tube lumen. We followed the distribution of several proteins normally secreted into tubular lumens to determine whether secretion was affected by loss of Dia and apical F-actin. Antibodies to the 2A12 antigen and to other secreted proteins normally detect secretion to the lumen of the trachea beginning at stage 13 of embryogenesis (Tsarouhas et al., 2007). The 2A12 antigen was absent from the lumen of the trachea in *dia* mutant embryos and following *dia* RNAi expression, and only traces could occasionally be detected within the cells comprising the smaller tubes (Figures 4A–4C).

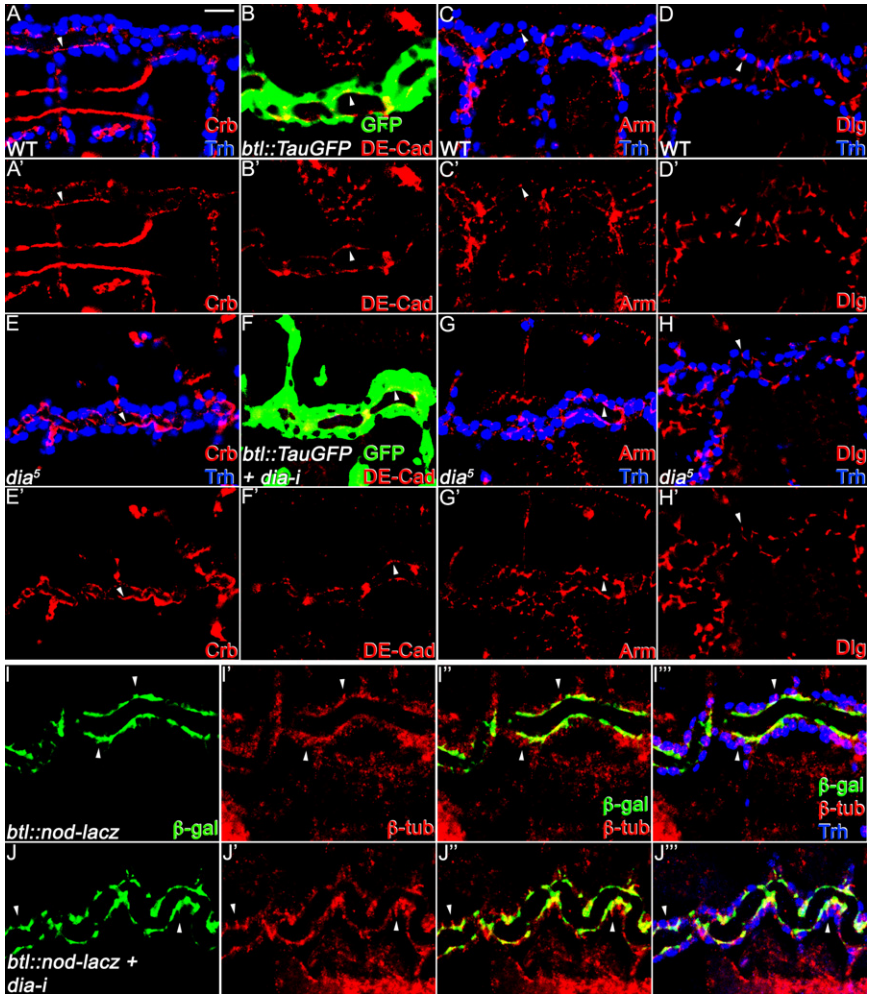


**Figure 2. Cell Polarity Is Maintained in *dia* Mutants**

The position of polarity and junctional markers (red, arrowheads) was examined in the tracheal dorsal trunk with respect to the position of the tracheal nuclei, marked by Trh (blue).

(A–D) Wild-type embryos showing the positions of the apical membrane protein, Crb, the adherens junctions marked by DE-Cad or Arm, and the septate junctions marked by Dlg. Scale bar, 10 μm.

(E–H) In *dia*$^{5}$ mutants, although the dorsal trunk is less regular, the markers maintain their normal positions.

(I–J‴) The apical position (arrowheads) of microtubule-minus ends and microtubules was determined with Nod-lacZ (green) and anti-β-tubulin (red), respectively, in wild-type embryos and following expression of *dia* RNAi VDRC20518.

The 2A12 antigen that failed to be secreted did not accumulate within the tracheal cells. To ascertain that the defect was indeed in secretion and not in synthesis of the 2A12 protein, we blocked trafficking to the lysosome by expressing an RNAi construct for *deep orange* (*dor*) (Sriram et al., 2003). When expressed alone in the trachea, accumulation of 2A12 in the lumen is normal and, in addition, some apical intracellular accumulation is also observed. When both *dor* and *dia* RNAi constructs were expressed, no secretion of 2A12 to the lumen was observed due to the absence of Dia, but apical accumulation within the tracheal cells was detected (Figures 4D and 4E). Accumulation of 2A12 antigen within the tracheal cells was also observed when a *dia* mutant was combined with a *sar1* mutant (encoding a subunit of the CopII trafficking complex), as a consequence of an early block in the secretory pathway ((Tsarouhas et al., 2007) and Figure S3). We can conclude that the 2A12 antigen is properly synthesized in the *dia* mutant background, but is rapidly targeted to degradation when a late step in secretion fails.

Another protein secreted by several tubular structures is the ZP-domain protein Piopio (Pio) (Figures 4F, 4K, and 4N and Jazwinska et al. [2003]). This protein contains a signal peptide and transmembrane domain, where the extracellular domain is constitutively cleaved upon maturation. Secreted Pio was shown to form a matrix within the lumen, together with the ZP-domain protein, Dumpy, generating a scaffold to support the migration of cells within the tube as they rearrange their positions and intercellular junctions (Jazwinska et al., 2003). In *dia* mutants, secretion of Pio is blocked in the trachea, hindgut, and salivary glands (Figures 4G, 4H, 4L, 4M, 4O, and 4P). Again, the Pio protein that failed to be secreted did not accumulate within the cells. Labeling of the tracheal cytoplasm of *dia* mutant embryos demonstrates discontinuities in the dorsal branches (Figures 4I and 4J and Figure S4F), resembling the *pio* mutant phenotype (Jazwinska et al., 2003). We also tested secretion of the ANF-GFP protein in the trachea (Tsarouhas et al., 2007), and observed loss of secretion in the absence of Dia (Figure S4). Thus, Dia appears to be required for apical secretion of multiple proteins.

The terminal cells of the trachea form a unique type of intracellular lumen (Ghabrial et al., 2003), which can be detected by antibodies directed against proteins, such as 2A12. The formation of this internal lumen is different from the lumens of the primary and secondary branches, where cells secrete material to the apical extracelullar space. While the cellular extensions of the terminal cells can be detected in *dia* mutant embryos, they do not contain the 2A12 antigen (Figure S4F), indicating that Dia is also required for the intracellular targeting of proteins toward the coalescing vesicles, that form the lumen of terminal cells.

## Dia Is Required for Secretion of a Distinct Class of Vesicles

Proper localization of Crb to the apical membrane of tracheal tubes in *dia* mutants while protein secretion to the lumen is blocked suggests that multiple routes are employed in trafficking protein cargo to the apical surface in these cells. Verm and Serp, chitin-modifying enzymes that are deposited in the tracheal lumen, were previously shown to require septate junctions for

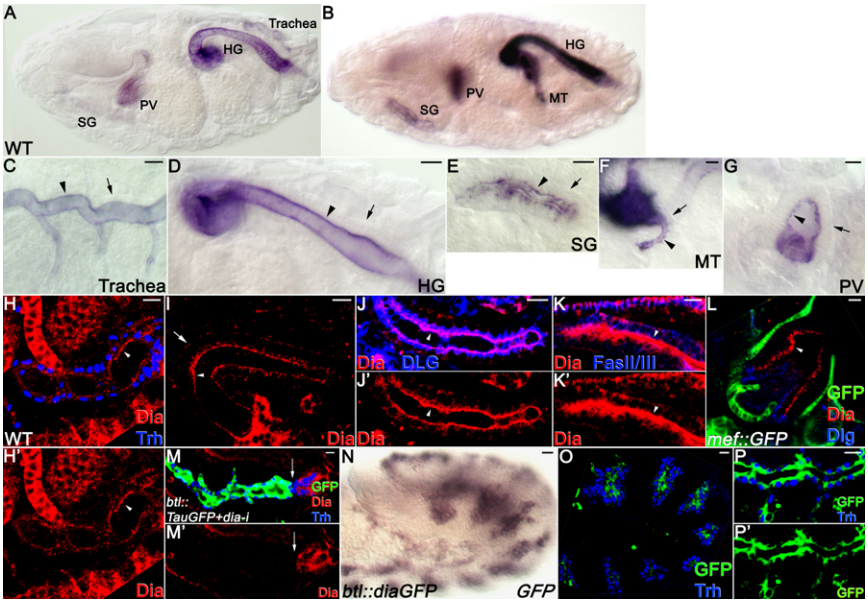


**Figure 3. *dia* mRNA and Protein Are Apically Localized in Diverse Tubular Organs**

(A and B) Starting at embryonic stage 14, *dia* mRNA begins to be detected predominantly in tubular organs, and this pattern becomes more prominent by stages 15 (A) and 16 (B).

(C–G) Within each one of the tubular organs, including trachea, hindgut, salivary glands, Malpighian tubules, and proventriculus, respectively, *dia* mRNA is localized to the apical side facing the tube lumen. In these and subsequent panels, arrowheads and arrows mark apical and basal surfaces, respectively. Scale bars, 10 μm.

(H–L) Staining the same tissues with anti-Dia demonstrates apical localization of the Dia protein. In contrast to the mRNA, protein generated at earlier stages perdures in other tissues, where it exhibits a nonpolarized distribution. Cell borders are marked in the salivary gland by Dlg (blue), and in Malpighian tubules by Fas II and III (blue). In (L), the muscle lining the outer layer of the proventriculus is marked with *mef2*-Gal4::*UAS-GFP*. Arrowheads and arrows mark apical and basal surfaces, respectively. Scale bars, 10 μm.

(M) Disappearance of Dia protein in the tracheal cells where *dia* RNAi (VDRC20518) is expressed, but not in the adjacent posterior spiracle cells (arrow). Scale bar, 10 μm.

(N) In embryos carrying *btl-Gal4*::*UAS-dia-GFP*, the localization of the ectopic transcript is followed by a probe for *GFP*, and shows a uniform distribution within the tracheal cells starting at stage 12. This indicates that the 3′UTR, which is lacking in the construct, is essential for apical localization of the *dia* transcript. Scale bar, 10 μm.

(O and P) The ectopic Dia-GFP protein was followed by staining for GFP (green), and shows a normal apical localization with respect to the tracheal nuclei (Trh, blue) at stages 12 and 15, respectively. Thus, an independent mechanism for apical localization of the Dia protein is utilized, even when the mRNA is not properly distributed. Scale bars, 10 μm.

their secretion. Compromising the structure of the septate junctions leads to failure to secrete these proteins to the lumen, while the secretion of 2A12 and Pio is unaffected (Luschnig et al., 2006; Wang et al., 2006). When we examined the secretion of the Verm and Serp proteins in a *dia* mutant background, we observed normal secretion (Figures 4Q–4S; Figures S3 and S4). This strengthens previous findings that the chitin-modifying enzymes are secreted by a distinct class of vesicles, which is not targeted apically. Dia is apparently required only for secretion of proteins that are packaged in apically secreted vesicles. The specific effect of *dia* mutants on secretion of a distinct class of vesicles, rather than a global effect on vesicle trafficking, was also ascertained by demonstrating a normal distribution of endoplasmic reticulum, Golgi, and recycling endosome markers (Figure S5), and normal endocytosis of Verm from the tracheal lumen at stage 17 (Figures 4T and 4U).

## Dia Is Activated Apically by Rho1 and Two Rho-GEFs

Activation of Dia-type Formins is commonly triggered by Rho and associated Rho-GEFs (Goode and Eck, 2007). We wanted to examine the localization and activity of these proteins, in the context of secretion by epithelial tube cells. The Rho1 protein shows an apical localization in tracheal tubes (Figure 5A). Furthermore, expression of PKNG58AeGFP, a GFP sensor for active Rho1 (Simoes et al., 2006), demonstrates that activation is apically restricted (Figure 5B). The Rho1 sensor can function as a Rho1-dominant negative, and its expression indeed leads to loss of 2A12 antigen secretion (Figure 5B). A similar effect is observed following expression of either Rho1 RNAi or dominant-negative constructs (Figures 5C and 5D), demonstrating the central role of Rho1 as a critical regulator of Dia. Since Rho1 is tethered to the membrane, its apical localization is particularly important in guiding polarized synthesis of F-actin by Dia. Thus, Dia will generate polarized actin cables, the barbed ends of which are embedded within the apical membrane.

The two Rho-GEFs, Gef2 and Gef64C, were previously shown to trigger Rho1 (Simoes et al., 2006). Both Gef2 and Gef64C display an apical protein localization in tracheal cells (Figures 5E and 5F). The apical localization of the pair of Rho-GEFs and Rho1 was also demonstrated in other tubular organs (Figure S6). When the level of Gef2 in the trachea was compromised by using a mutant background (Figure 5H), or by expression of an RNAi construct (Figure 6B), a block in secretion of 2A12 to the tracheal lumen was observed. Similar results were obtained in the *Gef64C* mutant background (Figure 5I), or following expression of *Gef64C* RNAi (Figure 6C), indicating that both Rho-GEFs are essential for apical secretion. Removal of one copy of either *Gef* gene has no effect (Figure S7). However, a strong block in secretion was observed in embryos that are transheterozygous for mutations in the two Rho-GEFs, (Figure 5J), suggesting that apical secretion requires a cumulative level of the two Rho-GEF proteins above a critical threshold. When present at sufficiently high levels, either GEF can drive 2A12 secretion, as demonstrated by the ability of Gef64C overexpression to rescue *Gef2* mutant or *Gef2* RNAi-expressing embryos (Figure S7). Markers of cell polarity display a normal

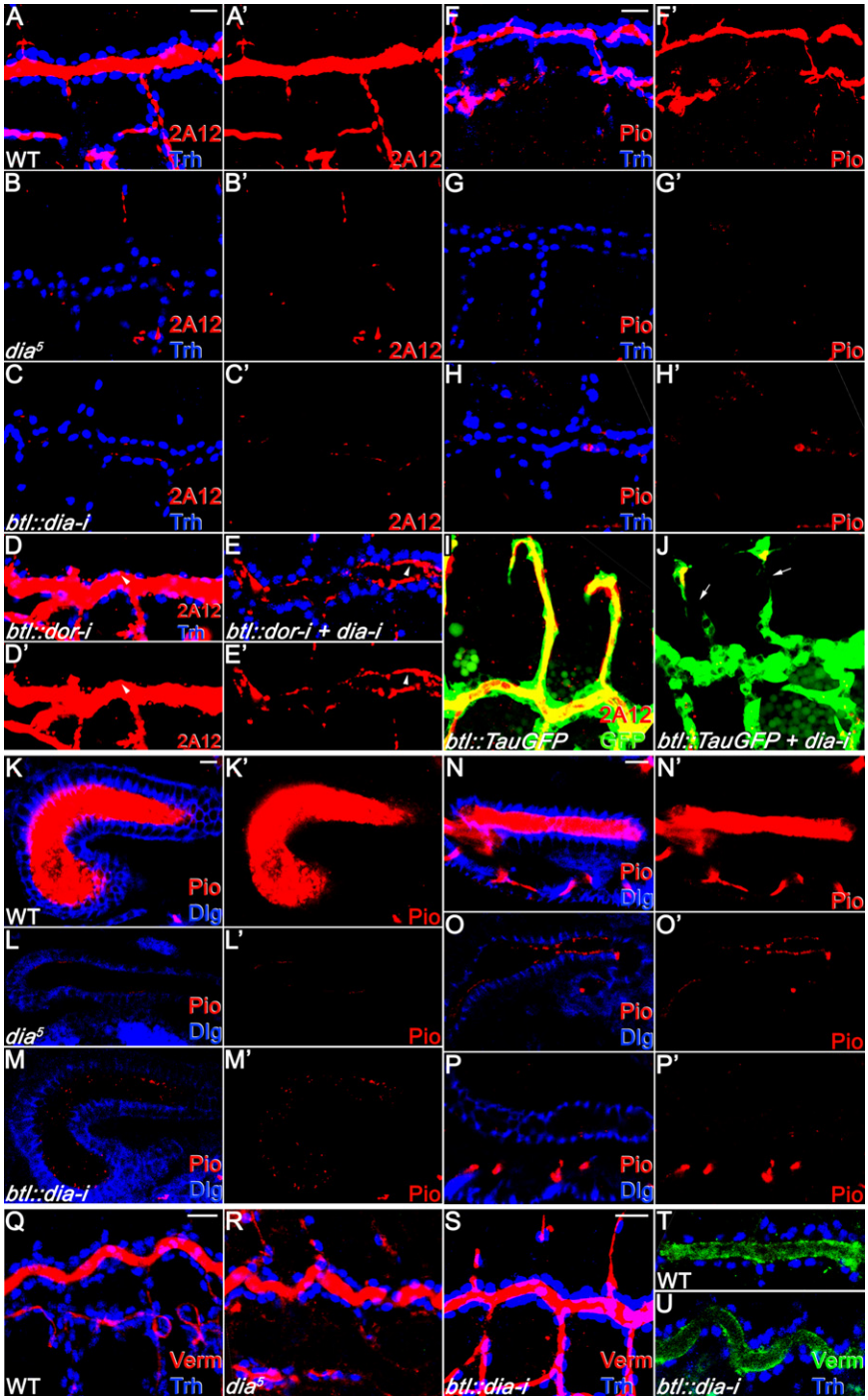


**Figure 4. Dia Is Required for Apical Secretion to the Lumen**

(A) In wild-type embryos, the 2A12 antigen (red) is secreted to the lumen of all tracheal tubes. Scale bar, 10 μm.

(B and C) In *dia*$^{5}$ mutant embryos, or *btl-Gal4* embryos expressing the VDRC20518 *dia* RNAi, the antigen is not deposited in the lumen, and does not accumulate within the tracheal cells. Occasionally, small patches of nonsecreted protein can be detected.

(D) Following expression of *dor* RNAi VDRC33734 in the trachea, secretion of 2A12 to the lumen is maintained, but accumulation of some antigen within the tracheal cells, apical to the nuclei, is observed (arrowhead).

(E) Upon coexpression of *dor* and *dia* RNAi, secretion of 2A12 to the lumen is blocked, but apical accumulation within the cells is detected (arrowhead).

(F) In wild-type embryos, the Pio ZP protein (red) is secreted to the tracheal lumen. Scale bar, 10 μm.

(G and H) No secretion or intracellular accumulation of Pio was detected in the two *dia* loss-of-function backgrounds tested above.

(I and J) Failure to secrete Pio in the absence of Dia leads to a tracheal phenotype reminiscent of *pio* mutant embryos (i.e., disruption of the junctions connecting the dorsal-branch cells [arrows]).

(K) Pio is normally secreted to the lumen of other tubular organs, which allows for examination of the requirement for Dia in additional tissues. In a wild-type embryo at stage 16, the hindgut lumen is filled with the Pio protein (cell junctions are marked by Dlg [blue]). Scale bar, 10 μm.

(L and M) In a *dia* mutant or in *drm-Gal4* embryos driving VDRC20518 *dia* RNAi, secretion of Pio is blocked and the protein does not accumulate within the cells.

(N) Wild-type embryo showing secretion of Pio (red) to the salivary gland lumen. Dlg-blue.

(O and P) In mutant *dia* embryos of the genotypes noted above, only marginal secretion of Pio to the lumen was observed.

(Q) Verm protein (red) is secreted to the tracheal lumen through the septate junctions (Trh, blue). Scale bar, 10 μm.

(R and S) In *dia*$^{5}$ mutant embryos or following expression of VDRC20518 *dia* RNAi in the trachea by *btl-Gal4*, secretion of Verm was not impaired, indicating that Dia is required only for secretion through the apical membrane. Scale bar, 10 μm.

(T and U) Endocytosis of Verm (green) from the tracheal lumen at stage 17 is also normal following *dia* RNAi expression.

Prime panels display staining of only 2A12 or Pio.

distribution in *Rho1*, *Gef2*, or *Gef64C* RNAi-expressing embryos (Figure S8), as in *dia* mutants.

We also wanted to test whether compromising the activity of Rho-GEFs or Rho1 gives rise to defects in the immediate output of Dia activity, namely, the nucleation of apical F-actin. When RNAi constructs for *Gef2*, *Gef64C*, or *Rho1* were expressed in the trachea, hindgut, or salivary glands, loss of apical F-actin was observed concomitant with defects in secretion (Figure 6). These results strengthen the causal link between Dia-mediated actin polymerization and apical secretion.

## Dia Activation Determines the Onset of Secretion

We used Rho1$^{V14}$, an activated form of Rho1, to validate the functional hierarchy between the Rho-GEFs, Rho1 and Dia, in tracheal cells. No defects in tracheal development or secretion were observed following expression of Rho$^{V14}$ in wild-type embryos (Figure 5L), likely due to the restricted apical localization of the protein. Expression of the same construct rescued the secretion defect in *Gef2*- or *Gef64C*-RNAi-expressing embryos (Figure 5M and data not shown), but failed to do so in *dia*-RNAi-expressing embryos (Figure 5N), thus demonstrating

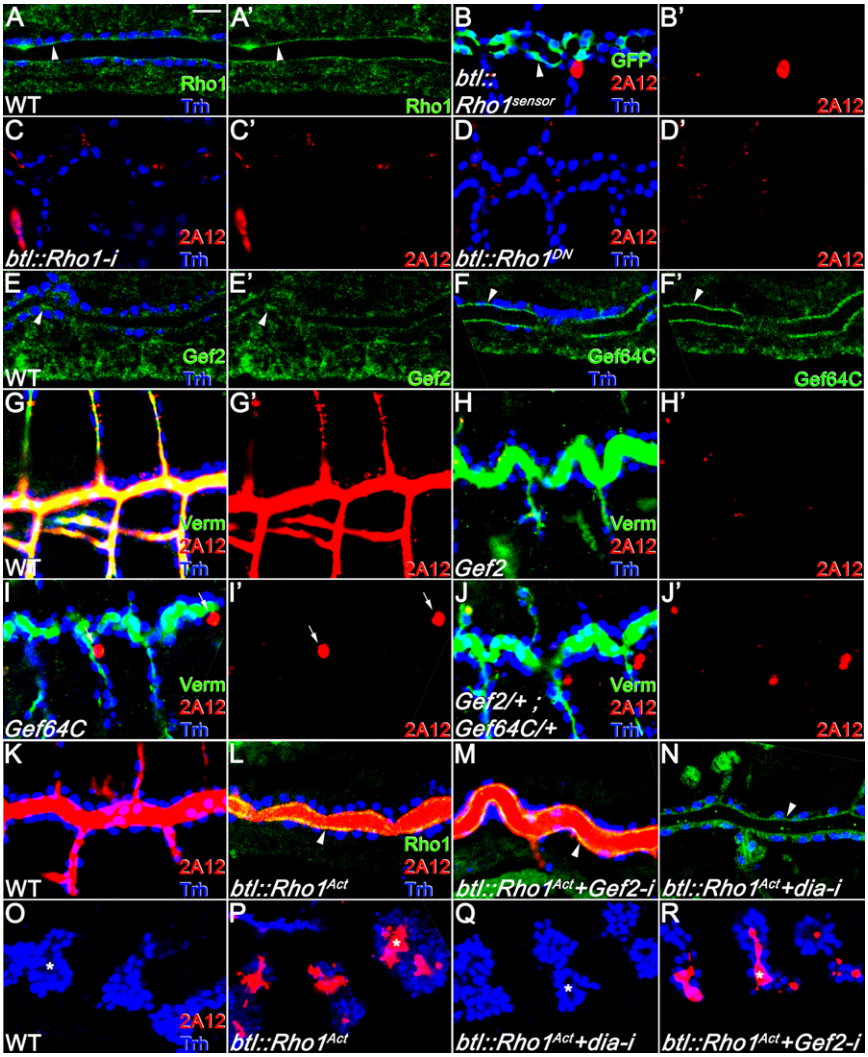


**Figure 5. Rho1 and Rho-GEFs Are Apically Localized and Trigger Dia**

(A) Rho1 (green) is apically localized in tubular structures of the trachea. Note that, in the adjacent, nontubular tissues, the protein is not polarized. Arrowheads mark apical surfaces. Scale bar, 10 μm.

(B) The active Rho sensor, PKNG58-eGFP (green), localizes apically following expression in trachea with *btl-Gal4*. Since the sensor functions as a dominant negative for Rho1, secretion of 2A12 (red) was blocked. Arrowhead marks apical surfaces.

(C and D) Expression of a *Rho1* RNAi VDRC12734 or $Rho1^{N19}$, a Rho1 dominant-negative construct, also blocked 2A12 secretion.

(E) Gef2 (green) is apically localized in the tracheal dorsal branch (Trh, blue). Arrowheads mark apical surfaces.

(F) Gef64C (green) is apically localized in the trachea. Arrowheads mark apical surfaces.

(G) Secretion was followed by 2A12 (red) and Verm (green). In a wild-type embryo, both accumulate in the lumen; (G′) shows only 2A12.

(H) In a *Gef2* mutant embryo, Verm was normally secreted, but no secretion of 2A12 was detected ([H′]2A12 channel).

(I) A similar result was observed in *Gef64C* mutant embryos. The clusters of 2A12 staining mark the cells of the spiracular branch, which accumulate the protein intracellularly at stage 16 (arrows).

(J) In a transheterozygous embryo of the genotype $Gef2^{-}$/+; $Gef64C^{-}$/+, no secretion of 2A12 was observed. This indicates that the two Rho-GEF proteins have similar functions, but must accumulate to a critical level in order to trigger Rho1.

(K) Wild-type (2A12, red; Trh, blue).

(L) Activated Rho1 was expressed by *btl-Gal4*. When monitored in the trachea at stage 15, the ectopic protein (expressed at higher levels than the endogenous Rho1) shows normal apical localization (Rho1, green; Trh, blue; 2A12, red). Arrowheads mark apical surfaces.

(M) Similar expression of activated Rho1 in a *Gef2* RNAi NIG9635R-3 background shows rescue of 2A12 secretion (red), indicating that activated Rho1 can bypass activation by Rho-GEFs. Arrowheads mark apical surfaces.

(N) Similar expression of activated Rho1 in a VDRC20518 *dia* RNAi background shows normal apical localization of Rho1, but no rescue of 2A12 secretion (red). Arrowheads mark apical surfaces.

(O) Tracheal pits of wild-type embryos at stage 12 do not show accumulation or secretion of 2A12 (red; Trh, blue). Asterisk indicates apical position.

(P) When embryos of the genotype in (L) were followed at stage 11/12, premature secretion of 2A12 antigen to the lumen was detected. Asterisk indicates apical position.

(Q) This premature secretion depends on the activity of Dia, since it was not observed in a *dia* VDRC20518 RNAi mutant background. The results suggest that the schedule of Dia activation is determined by a threshold for activation of Rho1 by GEFs. Asterisk indicates apical position.

(R) Premature secretion by activated Rho1 does not depend on GEFs, and was observed in a *Gef2* NIG9635R-3 RNAi background. Asterisk indicates apical position.

the expected functional epistatic relationship between the three proteins.

Apical secretion of proteins, like 2A12 and Pio, in the trachea is temporally regulated and is observed long after the lumen of the tracheal pits is formed at stage 11, suggesting a regulatory switch for onset of secretion. The high sensitivity of the system to the levels of the two Rho-GEFs that activate Rho1, suggests that activation of Rho1 may provide such a trigger. To test this notion, we examined the effects of activated Rho1 at earlier stages of tracheal development. Secretion was initiated at early stages of tracheal formation, and could be readily detected already at stage 12 (Figure 5P). This premature apical secretion is dependent on activation of Dia, since no secretion was observed when activated Rho1 was expressed in the presence of RNAi for *dia* (Figure 5Q). Conversely, activated Rho1 continued to trigger premature secretion in *Gef2*- or *Gef64C*-RNAi-expressing embryos (Figure 5R and data not shown). These results suggest that, normally, the machinery for apical localization of the critical components is already operational at early stages of tube morphogenesis, but that the activation of Dia takes place only at a subsequent phase.

We wanted to examine if the mechanism of apical localization of Rho-GEFs, Rho1 and Dia, is dependent on, or facilitated by, the apical actin cables formed by Dia. When the localization of

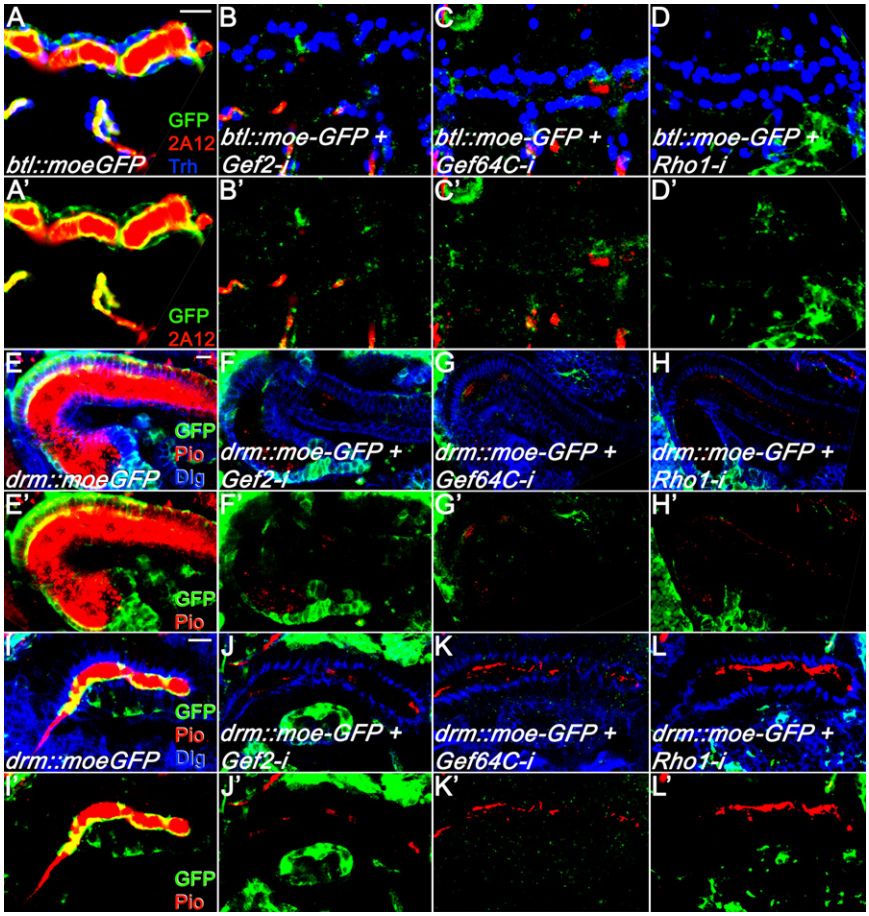


**Figure 6. Rho-GEFs and Rho1 Are Required for the Formation of Apical F-Actin in Tubular Structures**

F-actin was followed by Moe-GFP (green) to test if GEFs and Rho1 affect apical secretion through the formation of apical F-actin.

(A–D) 2A12 is secreted to the lumen of wild-type trachea, and apical F-actin is detected. When RNAi constructs for Gef2, Gef64C, or Rho1 were expressed by *btl-Gal4*, apical F-actin disappeared in parallel to the block in 2A12 secretion (Trh, blue; 2A12, red). Scale bar, 10 μm.

(E–H) In a wild-type embryo, Pio is secreted to the hindgut lumen and F-actin is detected both apically and basally. Expression of the above RNAi constructs by *drm-Gal4* abolished Pio secretion and accumulation of F-actin (Dlg, blue; Pio, red). Scale bar, 10 μm.

(I–L) In a wild-type embryo, Pio is secreted to the salivary gland lumen and F-actin is apically localized. Expression of the above RNAi constructs by *drm-Gal4* significantly reduced Pio secretion and abolished apical F-actin accumulation (Dlg, blue; Pio, red).

Gef2, Gef64C, or Rho1 was examined in a *dia*-RNAi background, it was comparable to the normal distribution (Figure S6). Furthermore, Dia retains its normal apical distribution in a *Rho1*-RNAi background (Figure S6). Thus, the apical localization of the upstream Dia regulators, and of Dia itself, is independent of Dia activity.

### MyoV Transports Cargo Vesicles Apically on Actin Cables

The simultaneous disruption of apical actin organization and apically directed secretion in *dia* mutants suggests that the Dia-nucleated actin filaments serve as tracks for polarized secretion. The actin-based MyoV motors have been linked to polarized secretion in a variety of biological systems (Reck-Peterson et al., 2000). A single homolog (*myoV*) is found in *Drosophila* (Bonafe and Sellers, 1998; MacIver et al., 1998). To assess its role in tubular organ secretion, we specifically inactivated *myoV* in the tracheal system, hindgut, and salivary gland with two independent RNAi constructs or a dominant-negative MyoV construct (Li et al., 2007). While secretion of 2A12 and Pio was abolished in these organs, the apical distribution of F-actin was not perturbed (Figures 7A–7J). MyoV protein is detected in a punctate distribution, and is eliminated from the tracheal cells following expression of an RNAi construct by *btl-Gal4*. In the trachea of *myoV* mutant embryos that develop to late stages, absence of 2A12 secretion, but normal Verm secretion, is detected. Finally, localization of MyoV is not altered in *dia* mutants and vice versa, and cell polarity markers are normal in embryos expressing *myoV* RNAi in the trachea (Figure S9).

The functional connection between MyoV and the Dia pathway was demonstrated by the ability to block premature secretion in the trachea, which was induced by activated Rho1 or constitutively activated Dia (Somogyi and Rorth, 2004) following coexpression of a *myoV* RNAi construct (Figures 7K–7N). These observations are consistent with a scenario whereby MyoV acts as a motor for trafficking secreted vesicles apically along actin cables generated by Dia.

## DISCUSSION

Apical localization of F-actin is a general feature of tubular epithelial structures. It was observed in mammalian MDCK cells forming tubes in three-dimensional cell culture (O'Brien et al., 2002), in the cytoplasm underlying the apical membrane facing the lumen in mammalian secretory organs, such as the lacrimal gland (Jerdeva et al., 2005), and in the different epithelial tubes of the *Drosophila* embryo (Tsarouhas et al., 2007) (Figure 1; Figure S1). The lower level of gene duplication in *Drosophila*, and the ability to follow the consequences of targeted gene inactivation in the tubular structures, allowed us to identify the mechanism responsible for nucleating the actin terminal web at the apical side of epithelial tube cells. We demonstrate that Dia, which is known to promote the formation of linear actin filaments, is responsible for producing this actin network in *Drosophila* embryonic tubular structures. Despite differences in the diameter and function of the different tubular organs, the polarized apical actin cables formed by Dia appear to have a common role in trafficking secretory vesicles to the apical tube surface.

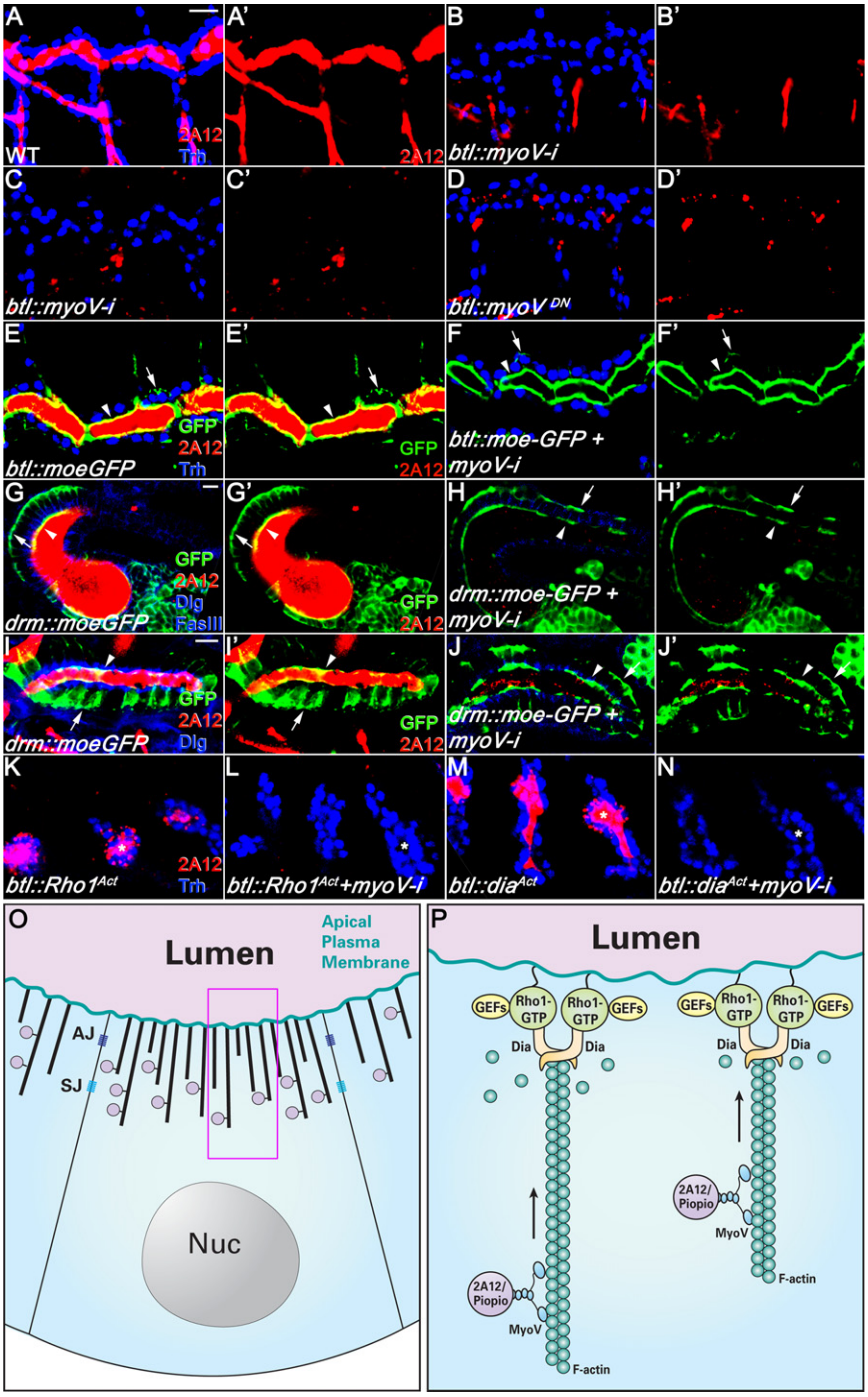


**Figure 7. MyoV Is Required for Apical Secretion in Tubular Structures**

(A–D) Secretion of 2A12 (red, Trh-blue) in the trachea of wild-type embryos (A) was compared to *btl-Gal4* embryos expressing *myoV* RNAi VDRC44291 (B), *myoV* RNAi (Li et al., 2007) (C), or a MyoV dominant-negative construct (D), are shown; 2A12 secretion to the lumen was blocked in all cases where MyoV activity was compromised; (A′)–(D′) show only the red channel. Scale bar, 10 μm.

(E and F) When Moe-GFP (green) was expressed in the trachea of wild-type or *myoV* RNAi VDRC44292 embryos, the apical F-actin was retained in the mutant; (E′) and (F′) show only green and red channels.

(G and H) The same experiments were carried out in the hindgut (Dlg, blue; Pio, red); (G′) and (H′) show only green and red channels. In a wild-type embryo, Pio is secreted to the hindgut lumen and F-actin is localized both apically and basally. When *myoV* RNAi was expressed by *drm-Gal4*, Pio was not secreted, but F-actin was retained. Scale bar, 10 μm.

(I and J) Similarly, the secretion of Pio and F-actin were monitored in the salivary glands, giving comparable results to the other tissues; (I′) and (J′) show only green and red channels. Arrowheads and arrows show apical and basal surfaces, respectively, in (E)–(H). Scale bar, 10 μm.

(K–N) Expression of activated Rho1 in the trachea leads to premature secretion of 2A12 (red) at stage 12, which is blocked by coexpression of *myoV* RNAi (VDRC44291) (L). Similar results were obtained following expression of activated Dia alone (M), or in combination with *myoV* RNAi (N). Asterisks show apical positions.

(O and P) Model for apical secretion in tubular structures. In diverse tubular structures, the single epithelial cell layer is highly polarized. Polarity is maintained by the adherens junction (AJ) and septate junction (SJ), forming tight barriers. Apical localization of the Dia activators (Rho-GEFs and Rho1), and Dia itself, promote the formation of polarized actin cables emanating from the apical membrane, with their barbed ends facing the membrane. This allows efficient trafficking by MyoV motors of a specific class of secretory vesicles toward the apical membrane. It is possible that, prior to loading of the vesicles onto MyoV motors and actin cables, they reach the general vicinity of the apical domain by microtubule-based mechanisms. (P) Magnified view of boxed area in (O).

While the role of Dia in promoting apical secretion spans the entire duration of tracheal morphogenesis, two other Formin-homology proteins act at very specific junctions of *Drosophila* tracheal morphogenesis. Formin 3 participates in the generation of a continuous dorsal trunk tube by promoting vesicular trafficking in the fusion cells of each metamer, perpendicular to the tube lumen (Tanaka et al., 2004). Another Formin domain protein, DAAM, promotes the organization of F-actin in rings around the circumference of the tracheal tube, at the final stages of tracheal morphogenesis (Matusek et al., 2006).

It is likely that each of the three Formin domain proteins is regulated by distinct activators that are concentrated at different sites. The localized activation of Formin 3 may eventually lead to polarized vesicle movement, similar to Dia, but toward a different membrane. The activation of DAAM may be necessary for the localized synthesis of F-actin, which will modify the contours of the apical membrane, and thus define the shape of chitin layered on top. The function of Dia stands out, since it is required throughout tracheal development, and is also involved in morphogenesis of other tubular organs.

### Multiple Tiers of Apical Localization Restrict Dia Activity to the Apical Surface

The mechanism of localized activation of Dia operates after apical-basal polarity of the cells has been established. Thus, we did not observe any defects in overall polarity in *dia* mutant embryos (Figure 2; Figure S2). It seems that the steps upstream to Dia activation utilize the existing polarity at multiple tiers in order to trigger Dia at a highly restricted position. The two Rho-GEF proteins, Gef2 and Gef64C, exhibit a tight apical localization in the cells forming the tubes. The single Rho1 protein, which is downstream to the Rho-GEFs, is again tightly localized to the apical surface in tubular structures (Figure 5). Binding of Rho1 to Dia leads to an opening of the autoinhibited form of Dia and to the formation of a Dia dimer representing the active form (Goode and Eck, 2007). Since GTP-bound Rho1 is the immediate activator of Dia, it is particularly important that Rho1 be embedded in the apical membrane, to ensure spatially restricted nucleation of actin polymerization. In *C. elegans*, a GEF and a Rho protein were shown to be essential for the development of the lumen of the excretory cell (Suzuki et al., 2001). It will be interesting to determine if a Dia-family protein is subsequently activated to promote secretion.

Dia is also apically localized, both at the mRNA and protein levels (Figure 3). Elimination of the *dia* 3′UTR demonstrated a persistence of apical protein localization, even when mRNA localization was lost, suggesting that there are two parallel and independent mechanisms for apical localization. The multiple tiers of apical localization assure that activated Dia will be highly restricted to the apical surface.

It is interesting to note that, while Gef2, Gef64C, Rho1, and Dia proteins are broadly expressed, partially due to maternal contribution of mRNA, they exhibit apical localization only in the tubular structures (Figures 3 and 5). This raises the possibility that genes that are specifically expressed in the tubular organs contribute to the apical localization. Alternatively, apical localization may rely directly on the specific phospholipid composition of the apical tube membranes. It will be interesting to determine if a common mechanism is responsible for the apical localization of the different proteins in the pathway, and if this mechanism relies on components that are restricted to the tubular organs.

The cellular machinery which dictates the apical localization of Rho-GEFs/Rho1/Dia appears to be in place early on. For example, expression of Dia-GFP in the trachea demonstrated apical localization of the protein already at the stage when the tracheal pits are formed (Figure 3P). Yet, generation of the polarized actin cables by Dia, and their utilization for secretion, takes place at a later stage, and follows a stereotypic temporal order in the different tracheal branches. What triggers activation of Dia, following the apical localization of the different components? We have demonstrated that both Gef2 and Gef64C are required to trigger Rho1, which activates Dia. While the activity of the two Rho-GEFs is similar, both have to accumulate to a critical level in order to activate the system (Figures 5H–5J). Thus, no secretion takes place when either of them is missing, or when each of them is present at half dose. The delay in activation of Dia and in secretion, may be explained by the time required to accumulate sufficient levels of Rho-GEF proteins. When the system was "short circuited" by expression of activated Rho1, which was properly localized to the apical surface, Dia-dependent apical secretion was observed already at early stages of tracheal pit formation (Figures 5P and 5Q).

### Cargo Vesicles Are Transported Apically on Actin Cables by MyoV

Our results identify *Drosophila* MyoV as a primary motor for apical trafficking of secretory vesicles along the polarized, Dia-nucleated actin cables in tubular organs. When the activity of MyoV was compromised in the tubular epithelia, apical secretion of cargos requiring Dia-generated actin cables was abolished. On the other hand, since MyoV operates downstream to Dia, the actin cables themselves remained intact (Figure 7). An analogous role for MyoV has been recently demonstrated during trafficking of Rhodopsins to photoreceptor rhabdomers (Li et al., 2007). The functional link between the Dia pathway and MyoV was demonstrated by the ability of *myoV* RNAi to suppress constitutively activated Rho1 or Dia phenotypes (Figures 7L and 7N). These results further support the direct link between Dia and apical secretion. A model describing the mechanism of Dia-regulated apical secretion in tubular organs is presented in Figures 7O and 7P.

The polarized actin network formed via the nucleating activity of Dia can account for the final phase of secretory vesicle transport to the apical plasma membrane. Class V myosins, such as MyoV, are known to be involved in transfer of vesicles from microtubules to cortical actin networks (Desnos et al., 2007), suggesting that polarized microtubule arrays may promote the long-range trafficking of the secretory vesicles from their sites of formation to the cell cortex. Consistent with this scenario, we have demonstrated a polarized arrangement of microtubules in tube epithelial cells, the minus ends of which are in close proximity to the apical membrane, which remains intact in the absence of Dia (Figure 2; Figure S2). The universality of this system is highlighted by similarities to polarized secretion in budding yeast, where Myo2p-mediated transport of secretory vesicles into the bud utilizes Dia-generated actin bundles as tracks, in order to deposit the compounds for polarized cell growth (Faix and Grosse, 2006).

### Actin Cables Promote the Apical Secretion of a Distinct Class of Vesicles

When early steps in the secretory pathway are compromised by reducing the activity of the COPII or COPI complexes, accumulation of cargo is observed within the cells and reduced amounts are detected in the lumen (Devine et al., 2005; Jayaram et al., 2008; Tsarouhas et al., 2007). Since these manipulations block an early and global process of secretion, all cargo vesicles are affected (Tsarouhas et al., 2007). However, after exit from the Golgi, it appears that distinct classes of vesicles are generated, each containing a different set of cargos, and trafficked by a distinct mechanism. One class of vesicles contains chitin-modifying enzymes (such as Verm or Serp), and is targeted to the septate junctions. When the structure of the septate junctions was compromised, these proteins failed to be secreted (Luschnig et al., 2006; Wang et al., 2006). Another class of vesicles may contain transmembrane proteins that are deposited in the apical membrane, such as Crb.

Our study now uncovers a third class of cargo vesicles. Several distinct cargos that are secreted to the apical lumen rely on Dia for

their secretion. These cargos include the 2A12 antigen, Pio, and the artificial rat ANF-GFP construct. In the absence of Dia, these proteins failed to be secreted to the lumen, but also did not accumulate within the epithelial tube cells (Figure 4; Figure S4). We believe that when secretion is disrupted, the vesicles are efficiently targeted for lysosomal degradation, since a block of lysosomal targeting facilitated intracellular accumulation of vesicles that failed to be secreted (Figure 4E). Inability to secrete Pio resulted in tracheal defects that were similar to *pio* mutant embryos. Additional defects of *dia* pathway mutant embryos, such as highly convoluted tracheal branches (compare Figures 2I and 2J), may stem from the absence of additional, yet unknown, proteins in the lumen. The mechanisms underlying the incorporation of distinct cargos into different secretory vesicles, as well as the recognition of each vesicle type by different motors and trafficking scaffolds, remain unknown.

In conclusion, this work has uncovered a universal mechanism, which operates in very different types of tubular epithelial structures in *Drosophila*. The conserved feature of an apical F-actin network in tubular epithelia of diverse multicellular organisms, and the high degree of conservation of the different components generating and utilizing these actin structures, strongly suggests that this polarized secretion mechanism is broadly used across phyla. The ability to generate polarized actin cables that initiate at the apical membrane provides an efficient route for trafficking vesicles by MyoV, leading to their fusion with the apical membrane and secretion. It is likely that different pathological situations manifested in aberrant formation of epithelial structures, or their utilization for secretion once the tubular organ is formed, represent defects in different components of this pathway. For example, it was shown that mutations in MyoVa in humans disrupt actin-based melanosome transport in epidermal melanocytes (Pastural et al., 1997).

## EXPERIMENTAL PROCEDURES

### Fly Strains

UAS-RNAi lines were as follows: *dia* (VDRC20518, NIG1768R-1), *Sop2* (VDRC42172), *Arp3* (VDRC35260), *dor* (VDRC33733, 33734), *Gef2* (NIG9635R-3), *Gef64C* (VDRC47121), *Rho1* (VDRC12734), *myoV* (VDRC44291, VDRC44292, RNAi flies from D. Ready [Li et al., 2007]). Other UAS lines include: *UAS-moe-GFP* (Chihara et al., 2003); *UAS-nod-lacZ* (Clark et al., 1997); *UAS-dia-GFP* (Homem and Peifer, 2008); *UAS-Dia CA* (activated) (Somogyi and Rorth, 2004); *UAS-serp-GFP* and *UAS-anf-GFP* (Tsarouhas et al., 2007); UAS-Rab11$^{SN}$ (dominant negative, provided by M. Gonzalez-Gaitan); *UAS-PKNG58eGFP* (active Rho1 sensor [Simoes et al., 2006]); *UAS-Rho1$^{N19}$* (DN); *UAS-Rho1$^{V14}$* (activated); *UAS-myoV-CT-GFP* (DN [Li et al., 2007]).

Mutants were as follows: *dia$^{5}$*, *Gef2$^{l(2)04291}$*, and *Gef64C$^{29}$*, PDI-GFP (Bobinnec et al., 2003), *myoV$^{Q1052st}$* (Li et al., 2007). *sar1$^{EP3575\Delta 28}$* (Tsarouhas et al., 2007) and *dar23$^{11\text{-}3\text{-}63}$* (Ye et al., 2007) represent different alleles of *sar1* and were used in a transheterozygous combination. Drivers were *btl-Gal4*, *drm-Gal4*, and *mef2-Gal4*.

The phenotypes observed following expression of RNAi constructs or in zygotic mutant backgrounds were highly consistent, but showed some variability, possibly due to fluctuation in the level of RNAi expression or the maternal mRNA contribution, respectively.

### Probes and Antibodies

Dig-labeled DNA probes for *dia* (nucleotide positions 12–676 or 2518–3228 in the coding region) and *GFP* (encompassing the entire coding region) were used for RNA in situ hybridization according to Melen et al. (2005). Antbodies include: Trh (rat 1:100), anti-GFP (chicken 1:500; Abcam); Crb, Arm, Dlg, Fas II, and Fas III (mouse 1:100; DSHB), DE-Cad (rat 1:100; DSHB), Dia-rabbit 1:250 (Grosshans et al., 2005), 2A12 (mouse IgM 1:5; DSHB), Pio-rabbit 1:100 (Jazwinska et al., 2003), Verm-guinea pig 1:200 (Wang et al., 2006), β-tubulin (mouse 1:500; Sigma), Golgi (dGMAP, rabbit 1:500; C. Rabouille), Rab11 (rabbit 1:50; M. Gonzalez-Gaitan), Gef2-rabbit 1:1000 (Grosshans et al., 2005), Gef64C-mouse 1:50 (Bashaw et al., 2001), Rho1-mouse 1:50 (Magie et al., 2002). Cy2, -3, and -5 secondary antibodies and biotin-conjugated goat-anti mouse IgM (for 2A12 antigen) were purchased from Jackson ImmunoResearch and diluted 1:200. For detection of IgM antibodies, streptavidin-HRP and TSA kit (Perkin-Elmer), followed by Cy-conjugated streptavidin, were used.

Standard fixation and staining procedures were followed. To detect Dia, GEFs, and Rho1, heat fixation was used: embryos were collected and bleached in a nylon mesh, immersed in 5 ml boiling 0.7% NaCl and 0.04% Triton X-100 for 10 s, and vortexed briefly. Cold solution (20 ml) was quickly added, and embryos chilled on ice before devitellinization in heptane/methanol. EM procedure was carried out according to (Massarwa et al., 2007).

## SUPPLEMENTAL DATA

Supplemental Data include nine figures and can be found with this article online at http://www.cell.com/developmental-cell/supplemental/S1534-5807(09)00172-5/.

## ACKNOWLEDGMENTS

We thank the following scientists and organizations for generously providing fly strains and antibodies: M. Affolter, Y. Bobinnec, M. Gonzalez-Gaitan, J. Grösshans, S. Hayashi, A. Jacinto, Y. Jan, M. Peifer, C. Rabouille, D. Ready, P. Rorth, C. Samakovlis, Vienna *Drosophila* RNAi Center, National Institute of Genetics (Japan), the Developmental Studies Hybridoma Bank, and the Bloomington *Drosophila* stock center. We thank S. Yogev for helpful discussions. The work was funded by grants from the Israel Science Foundations (to E.D.S. and B.-Z.S.) and Nissim Foundation (B.-Z.S.). B.-Z.S. is an incumbent of the Hilda and Cecil Lewis chair for Molecular Genetics.

Received: December 10, 2008
Revised: March 15, 2009
Accepted: April 21, 2009
Published: June 15, 2009

## REFERENCES

Bashaw, G.J., Hu, H., Nobes, C.D., and Goodman, C.S. (2001). A novel Dbl family RhoGEF promotes Rho-dependent axon attraction to the central nervous system midline in *Drosophila* and overcomes Robo repulsion. J. Cell Biol. *155*, 1117–1122.

Beitel, G.J., and Krasnow, M.A. (2000). Genetic control of epithelial tube size in the *Drosophila* tracheal system. Development *127*, 3271–3282.

Bobinnec, Y., Marcaillou, C., Morin, X., and Debec, A. (2003). Dynamics of the endoplasmic reticulum during early development of *Drosophila* melanogaster. Cell Motil. Cytoskeleton *54*, 217–225.

Bonafe, N., and Sellers, J.R. (1998). Molecular characterization of myosin V from *Drosophila* melanogaster. J. Muscle Res. Cell Motil. *19*, 129–141.

Bryant, D.M., and Mostov, K.E. (2008). From cells to organs: building polarized tissue. Nat. Rev. Mol. Cell Biol. *9*, 887–901.

Buechner, M., Hall, D.H., Bhatt, H., and Hedgecock, E.M. (1999). Cystic canal mutants in *Caenorhabditis elegans* are defective in the apical membrane domain of the renal (excretory) cell. Dev. Biol. *214*, 227–241.

Chihara, T., Kato, K., Taniguchi, M., Ng, J., and Hayashi, S. (2003). Rac promotes epithelial cell rearrangement during tracheal tubulogenesis in *Drosophila*. Development *130*, 1419–1428.

Clark, I.E., Jan, L.Y., and Jan, Y.N. (1997). Reciprocal localization of Nod and kinesin fusion proteins indicates microtubule polarity in the *Drosophila* oocyte, epithelium, neuron and muscle. Development *124*, 461–470.

Desnos, C., Huet, S., and Darchen, F. (2007). 'Should I stay or should I go?': myosin V function in organelle trafficking. Biol. Cell *99*, 411–423.

Devine, W.P., Lubarsky, B., Shaw, K., Luschnig, S., Messina, L., and Krasnow, M.A. (2005). Requirement for chitin biosynthesis in epithelial tube morphogenesis. Proc. Natl. Acad. Sci. USA *102*, 17014–17019.

Faix, J., and Grosse, R. (2006). Staying in shape with formins. Dev. Cell *10*, 693–706.

Ghabrial, A., Luschnig, S., Metzstein, M.M., and Krasnow, M.A. (2003). Branching morphogenesis of the *Drosophila* tracheal system. Annu. Rev. Cell Dev. Biol. *19*, 623–647.

Goode, B.L., and Eck, M.J. (2007). Mechanism and function of formins in the control of actin assembly. Annu. Rev. Biochem. *76*, 593–627.

Grosshans, J., Wenzl, C., Herz, H.M., Bartoszewski, S., Schnorrer, F., Vogt, N., Schwarz, H., and Muller, H.A. (2005). RhoGEF2 and the formin Dia control the formation of the furrow canal by directed actin assembly during *Drosophila* cellularisation. Development *132*, 1009–1020.

Hartenstein, V. (1993). Atlas of *Drosophila Development* (Cold Spring Harbor, NY: Cold Spring Harbor Laboratory Press).

Hemphala, J., Uv, A., Cantera, R., Bray, S., and Samakovlis, C. (2003). Grainy head controls apical membrane growth and tube elongation in response to Branchless/FGF signalling. Development *130*, 249–258.

Hogan, B.L., and Kolodziej, P.A. (2002). Organogenesis: molecular mechanisms of tubulogenesis. Nat. Rev. Genet. *3*, 513–523.

Homem, C.C., and Peifer, M. (2008). Diaphanous regulates myosin and adherens junctions to control cell contractility and protrusive behavior during morphogenesis. Development *135*, 1005–1018.

Jayaram, S.A., Senti, K.A., Tiklova, K., Tsarouhas, V., Hemphala, J., and Samakovlis, C. (2008). COPI vesicle transport is a common requirement for tube expansion in *Drosophila*. PLoS ONE *3*, e1964. 10.1371/journal.pone.0001964.

Jazwinska, A., Ribeiro, C., and Affolter, M. (2003). Epithelial tube morphogenesis during *Drosophila* tracheal development requires Piopio, a luminal ZP protein. Nat. Cell Biol. *5*, 895–901.

Jerdeva, G.V., Wu, K., Yarber, F.A., Rhodes, C.J., Kalman, D., Schechter, J.E., and Hamm-Alvarez, S.F. (2005). Actin and non-muscle myosin II facilitate apical exocytosis of tear proteins in rabbit lacrimal acinar epithelial cells. J. Cell Sci. *118*, 4797–4812.

Kerman, B.E., Cheshire, A.M., and Andrew, D.J. (2006). From fate to function: the *Drosophila* trachea and salivary gland as models for tubulogenesis. Differentiation *74*, 326–348.

Li, B.X., Satoh, A.K., and Ready, D.F. (2007). Myosin V, Rab11, and dRip11 direct apical secretion and cellular morphogenesis in developing *Drosophila* photoreceptors. J. Cell Biol. *177*, 659–669.

Lubarsky, B., and Krasnow, M.A. (2003). Tube morphogenesis: making and shaping biological tubes. Cell *112*, 19–28.

Luschnig, S., Batz, T., Armbruster, K., and Krasnow, M.A. (2006). serpentine and vermiform encode matrix proteins with chitin binding and deacetylation domains that limit tracheal tube length in *Drosophila*. Curr. Biol. *16*, 186–194.

MacIver, B., McCormack, A., Slee, R., and Bownes, M. (1998). Identification of an essential gene encoding a class-V unconventional myosin in *Drosophila melanogaster*. Eur. J. Biochem. *257*, 529–537.

Magie, C.R., Pinto-Santini, D., and Parkhurst, S.M. (2002). Rho1 interacts with p120ctn and alpha-catenin, and regulates cadherin-based adherens junction components in *Drosophila*. Development *129*, 3771–3782.

Massarwa, R., Carmon, S., Shilo, B.Z., and Schejter, E.D. (2007). WIP/WASp-based actin-polymerization machinery is essential for myoblast fusion in *Drosophila*. Dev. Cell *12*, 557–569.

Matusek, T., Djiane, A., Jankovics, F., Brunner, D., Mlodzik, M., and Mihaly, J. (2006). The *Drosophila* formin DAAM regulates the tracheal cuticle pattern through organizing the actin cytoskeleton. Development *133*, 957–966.

Melen, G.J., Levy, S., Barkai, N., and Shilo, B.Z. (2005). Threshold responses to morphogen gradients by zero-order ultrasensitivity. Mol. Syst. Biol. *1*, 2005.0028. 10.1038/msb4100036.

Myat, M.M., and Andrew, D.J. (2002). Epithelial tube morphology is determined by the polarized growth and delivery of apical membrane. Cell *111*, 879–891.

O'Brien, L.E., Zegers, M.M., and Mostov, K.E. (2002). Opinion: building epithelial architecture: insights from three-dimensional culture models. Nat. Rev. Mol. Cell Biol. *3*, 531–537.

Pastural, E., Barrat, F.J., Dufourcq-Lagelouse, R., Certain, S., Sanal, O., Jabado, N., Seger, R., Griscelli, C., Fischer, A., and de Saint Basile, G. (1997). Griscelli disease maps to chromosome 15q21 and is associated with mutations in the myosin-Va gene. Nat. Genet. *16*, 289–292.

Reck-Peterson, S.L., Provance, D.W., Jr., Mooseker, M.S., and Mercer, J.A. (2000). Class V myosins. Biochim. Biophys. Acta *1496*, 36–51.

Simoes, S., Denholm, B., Azevedo, D., Sotillos, S., Martin, P., Skaer, H., Hombria, J.C., and Jacinto, A. (2006). Compartmentalisation of Rho regulators directs cell invagination during tissue morphogenesis. Development *133*, 4257–4267.

Somogyi, K., and Rorth, P. (2004). Evidence for tension-based regulation of *Drosophila* MAL and SRF during invasive cell migration. Dev. Cell *7*, 85–93.

Sriram, V., Krishnan, K.S., and Mayor, S. (2003). deep-orange and carnation define distinct stages in late endosomal biogenesis in *Drosophila melanogaster*. J. Cell Biol. *161*, 593–607.

Suzuki, N., Buechner, M., Nishiwaki, K., Hall, D.H., Nakanishi, H., Takai, Y., Hisamoto, N., and Matsumoto, K. (2001). A putative GDP-GTP exchange factor is required for development of the excretory cell in *Caenorhabditis elegans*. EMBO Rep. *2*, 530–535.

Tanaka, H., Takasu, E., Aigaki, T., Kato, K., Hayashi, S., and Nose, A. (2004). Formin3 is required for assembly of the F-actin structure that mediates tracheal fusion in *Drosophila*. Dev. Biol. *274*, 413–425.

Tsarouhas, V., Senti, K.A., Jayaram, S.A., Tiklova, K., Hemphala, J., Adler, J., and Samakovlis, C. (2007). Sequential pulses of apical epithelial secretion and endocytosis drive airway maturation in *Drosophila*. Dev. Cell *13*, 214–225.

Wang, S., Jayaram, S.A., Hemphala, J., Senti, K.A., Tsarouhas, V., Jin, H., and Samakovlis, C. (2006). Septate-junction-dependent luminal deposition of chitin deacetylases restricts tube elongation in the *Drosophila* trachea. Curr. Biol. *16*, 180–185.

Wu, K., Jerdeva, G.V., da Costa, S.R., Sou, E., Schechter, J.E., and Hamm-Alvarez, S.F. (2006). Molecular mechanisms of lacrimal acinar secretory vesicle exocytosis. Exp. Eye Res. *83*, 84–96.

Ye, B., Zhang, Y., Song, W., Younger, S.H., Jan, L.Y., and Jan, Y.N. (2007). Growing dendrites and axons differ in their reliance on the secretory pathway. Cell *130*, 717–729.